# Elucidation and visualization of solid-state transformation and mixing in a pharmaceutical mini hot melt extrusion process using in-line Raman spectroscopy

Jeroen Van Renterghem[1*], Ashish Kumar[2], Chris Vervaet[3], Jean Paul Remon[3], Ingmar Nopens[2], Yvan Vander Heyden[4], Thomas De Beer[1]

[1] Laboratory of Process Analytical Technology, Ghent University, Ottergemsesteenweg 460, 9000 Ghent, Belgium

[2] BIOMATH, Ghent University, Coupure Links 653, 9000 Ghent, Belgium

[3] Laboratory of Pharmaceutical Technology, Ghent University, Ottergemsesteenweg 460, 9000 Ghent, Belgium

[4] Dept of Analytical Chemistry and Pharmaceutical Technology, VUB, Laarbeeklaan 103, 1090 Brussels, Belgium

*Corresponding author: Jeroen Van Renterghem

Laboratory of Process Analytical Technology, Ghent University, Ottergemsesteenweg 460, 9000 Ghent, Belgium

TEL: 0032 9 264 8039

FAX: 0032 9 264

E-MAIL: jeroen.vanrenterghem@ugent.be

Abstract

Mixing of raw materials (drug + polymer) in the investigated mini pharma melt extruder is achieved by using co-rotating conical twin screws and an internal recirculation channel. In-line Raman spectroscopy was implemented in the barrels, allowing monitoring of the melt during processing. The aim of this study was twofold: to investigate (I) the influence of key process parameters (screw speed - barrel temperature) upon the product solid-state transformation during processing of a sustained release formulation in recirculation mode; (II) the influence of process parameters (screw speed - barrel temperature - recirculation time) upon mixing of a crystalline drug (tracer) in an amorphous polymer carrier by means of residence time distribution (RTD) measurements. The results indicated a faster mixing endpoint with increasing screw speed. Processing a high drug load formulation above the drug melting temperature resulted in the production of amorphous drug whereas processing below the drug melting point produced solid dispersions with partially amorphous/crystalline drug. Furthermore, increasing the screw speed resulted in lower drug crystallinity of the solid dispersion. RTD measurements elucidated the improved mixing capacity when using the recirculation channel. In-line Raman spectroscopy has shown to be an adequate PAT-tool for product solid-state monitoring and elucidation of the mixing behavior during processing in a mini extruder.

Keywords: hot-melt extrusion, Raman spectroscopy, solid-state transformation, residence time distribution, mixing, transport, recirculation time

Graphical abstract

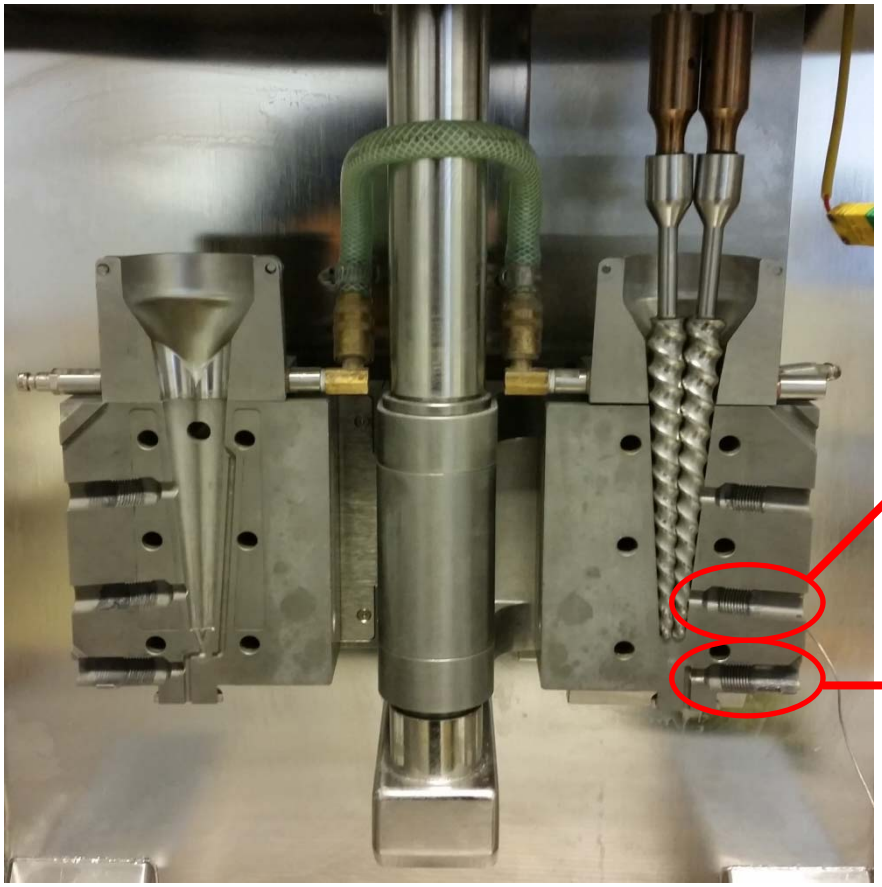

RAMAN spectroscopy

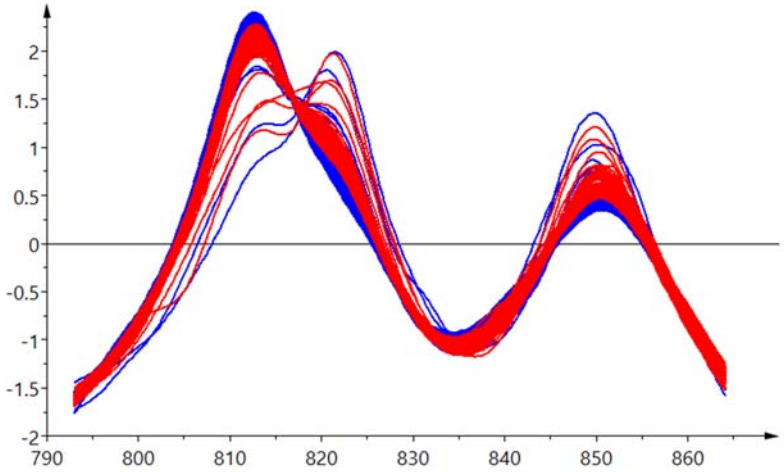


Solid-state transformation analysis

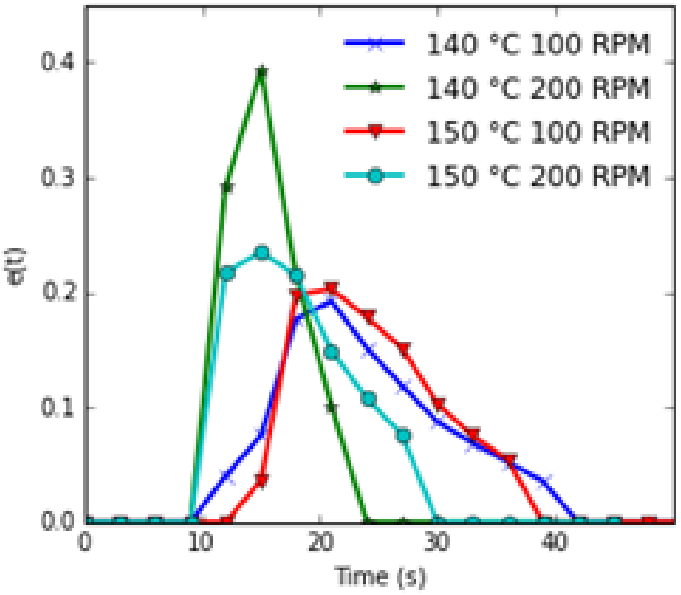


Residence time distribution measurements

# 1 Introduction

New active pharmaceutical ingredients (API) are often very expensive and available in limited quantity (only a few grams) at the early stage of formulation development. Moreover, laboratory-scale extruders require large amounts of drug substance and matrix products as their throughputs are in the range of kg/h (e.g. 16mm Eurolab, Thermo Fisher Scientific). Nowadays, mini pharmaceutical hot-melt extruders (grams per batch) are available for the pharmaceutical industry to allow cost effective screening in formulation development. This throughput can be reduced somewhat by using supercritical CO2 as a diluent (Verreck et al., 2006; Vigh et al., 2014b). A mini extruder consists of co-rotating conical twin-screws and an internal recirculation channel to achieve (complete) mixing of the raw materials (drug substance + matrix). The design of a mini extruder is mostly fixed (i.e., screw design), therefore a recirculation channel is provided to improve distributive mixing. This is completely different compared to lab-scale extruders, since their segmental screw design allows to adjust the screw configuration to improve distributive mixing. The intended purpose of a hot-melt extruder is to homogenously mix the raw materials until the desired solid dispersion is obtained. The degree of mixing required between the drug and the polymer matrix may depend on the type of solid dispersion (i.e., product solid-state: e.g. molecularly dispersed or crystalline dispersed drug in an amorphous polymer matrix), the properties (e.g. drug melting temperature, miscibility) of the components, the formulation composition and the Quality Target Product Profile (QTPP) (Sakai and Thommes, 2014). The final solid-state of the drug product is determined by the processing history. Hence, the product solid-state is altered by

the main process parameters in a mini extrusion process: screw speed, barrel temperature and recirculation time.

The QbD/PAT initiative (Administration, 2004) supports bottom-up formulation and process development, for instance by using process analyzers, also at a small scale. Since real-time data collection of the melt properties (e.g., solid-state) during processing is possible via spectroscopic techniques, the influence of process factors upon the critical quality attributes (CQA) (such as, solid-state, melt homogeneity) can be visualized during processing. Furthermore, information of material and processing behavior gathered on the small scale extruder could be used for later scale-up towards laboratory and industrial scale hot-melt extruders. Immersion probes connected via fiber optical cables to spectrometers can be implemented in the hot-melt extrusion process stream for real-time monitoring of the melt. In-line Raman and NIR analyzers are complementary techniques (De Beer et al., 2011) already used in laboratory-scale hot-melt extruders to improve understanding of the material and processing behavior. Saerens et al. visualized the material behavior in the extrusion barrel (along the entire length) using Raman spectroscopy to gain process understanding of a laboratory-scale extrusion process (Eurolab 16mm, Thermo Fisher Scientific) (Saerens et al., 2013). The influence of key process parameters (screw speed and barrel temperature) could be linked with the product solid-state and drug-polymer interactions. Since the product solid-state was monitored along the entire extruder barrel length, it was possible to determine the barrel segment where the final product solid-state was formed. Comparison between Raman spectra of the physical mixtures and the in-line collected spectra showed Raman peak shifts, which were attributed to the chemical interactions between drug and polymer. Raman spectrometry allows to predict the properties of melt extruded solid dispersion (Vigh et al., 2014a). Also NIR diffuse reflectance spectroscopy showed these spectral shifts and proved to

be an adequate PAT-tool to visualize the drug-polymer interactions during processing (Saerens et al., 2012). However, NIR diffuse reflectance spectroscopy showed larger noise levels when monitoring transparent samples compared to opaque samples. Therefore, transmission NIR spectroscopy was used by Islam et al. to monitor the drug (Indometacine) transformation (i.e., solid-state change) when mixing with Kollidon VA64 and Soluplus (Islam et al., 2015). To our knowledge, no attempt was made so far to implement spectroscopic techniques in a mini-extruder of this type. Raman backscattering spectroscopy was chosen as a monitoring technique because of the ease of implementation in the splittable and removable barrel-liners and because it provided a good signal for both transparent and opaque samples.

In-line process analyzers (Raman and NIR spectroscopy) are fast measuring techniques that are ideal for real-time data collection as no sample pretreatment is necessary (De Beer et al., 2011). This advantage over slow offline techniques (e.g. HPLC) is helpful to study the melt flow behavior and mixing during processing. Often the residence time distribution (RTD) of a tracer molecule is measured to elucidate the mixing capacity of the mixing device under investigation. In-line Raman spectroscopy was used by Common et al. for residence time measurements in a single screw extrusion process (Common et al., 2014). Their research elucidated the improved mixing capacity of adding a static mixer between the screw and die. In contrast to their research, the in this study investigated mini-extruder has a recirculation channel to improve distributive mixing. Not only the recirculation channel, but also the screw speed and barrel temperature could influence the melt flow behavior and thus the mixing degree (i.e., mixing endpoint) of the tracer molecule with the polymer matrix. To our best knowledge, the use of RTD measurements has not yet been described in literature to examine the influence of the recirculation channel upon the mixing capacity and the melt flow behavior in a mini extruder of this type.

The aim of this study was twofold: (i) to investigate the influence of key process parameters (screw speed and barrel temperature) upon the product solid-state during processing of a sustained release formulation in a pharmaceutical mini hot-melt extruder using in-line Raman spectroscopy, (ii) to elucidate the influence of process parameters (screw speed, barrel temperature and recirculation time) upon the mixing capacity by means of RTD measurements (measured via in-line Raman spectroscopy) when processing a crystalline drug (tracer molecule) in an amorphous polymer matrix.

# 2 Materials and methods

## 2.1 Influence of process parameters on product solid-state

### 2.1.1 Hot-melt extrusion: pharmaceutical formulation and experimental setup

Physical mixtures containing 10 and 40 % w/w Metoprolol tartrate (MPT) (Esteve Quimica, Barcelona, Spain) in Eudragit® RS PO (Evonik, Germany) were prepared with a mortar and pestle. The melting temperature ($T_m$) of MPT is 120°C. Eudragit® RS PO is a copolymer of ethyl acrylate, methyl methacrylate and a low content of methacrylic acid ester with quaternary ammonium groups. It is an amorphous polymer with a glass transition temperature ($T_g$) of 65°C that shows good miscibility with MPT (Saerens et al., 2013). The physical mixtures (6g) were manually fed and extruded with an Xplore Pharma Micro Extruder (PME5, Xplore Instruments, Geleen, Netherlands) with a 5 ml splittable barrel (Fig 1). The extrusion process was carried out in recirculation mode. Screw speed (25 - 50 rpm) and barrel temperature (105 - 140°C) were varied, resulting in a total of 8 experiments. The relatively

narrow range of screw speeds was selected based on practical considerations. Higher screw speeds could potentially damage the probe's sapphire window since the screws are very close to the immersion probe (position 2, Fig 1). The logged data (i.e., barrel temperature, screw speed, normal force) from the mini extruder was captured by the Micro Compounder v10.1 software.

### 2.1.2 In-line Raman spectroscopy: data acquisition and post processing

A Raman dynisco probe was implemented at position 2 in the splittable barrel, shown in figure 1. The probe was connected via a fiber optical cable to the Rxn2 Raman spectrometer (Kaiser optical systems, Washington, USA), equipped with a CCD detector. The employed laser wavelength was 785 nm. In-line Raman spectra were collected every 5 s with an acquisition time of 3 s for a duration of 15 minutes. The collected Raman spectra were analyzed using Simca 13.0.3 (Umetrics, Umeå, Sweden). Spectra were preprocessed with SNV (to compensate for scatter-induced baseline shifts) and mean centering prior to principal component analysis (PCA).

### 2.1.3 Differential scanning calorimetry (DSC)

All obtained extrudates and physical mixtures were measured with a DSC Q 2000 (TA instruments, Belgium). Extrudate and physical mixture samples were prepared and measured

with hermetic sealed aluminum pans. Measurements were carried out in a nitrogen atmosphere with a heating rate of 10 °C/min. Thermograms were produced with the Thermal Advantage Release 5.1.2 software. The first heating was analyzed using TA Instruments Universal Analysis 2000 4.5A software.

## 2.2 Residence time analysis: experimental design and data analysis

### 2.2.1 Raw materials

Eudragit® RS PO was also used as a polymer matrix during RTD measurements. Theophylline anhydrous powder 200M (BASF) was used as tracer molecule. The tracer molecule is expected to remain crystalline during processing since the melting temperature (Tm) is much higher (Tm = ±270°C) than the processing temperatures during the RTD experiments.

### 2.2.2 Hot-melt extrusion RTD experimental setup

During each experiment, pure Eudragit® RS PO (5g) was manually fed into the mini extruder and then further processed during 1 minute (using the recirculation channel) to obtain a steady state based on equilibration of the extruder's logged normal force prior to the addition of the tracer (0.5g). The recirculation time after the addition of the tracer was varied between 0 and 90 s with 15 s increment using a turning valve (switching from recirculation mode to continuous mode). At the moment the valve was turned to continuous mode, pure

Eudragit® RS PO was fed to push the processed material out of the barrel. The influence of two factors, screw speed (100 - 200 rpm) and barrel temperature (140 - 150 °C), upon RTD and hence mixing was examined using a 2-level full factorial experimental design. This experimental setup resulted in a total of 49 RTD measurements (i.e., 7 recirculation times × (2 factors at 2 levels ($2^2$) + 3 replicates at the center point)). The information from the replicate measurements was used to estimate the experimental error in the determination of the significance of factor and interaction effects.

### 2.2.3 Raman spectroscopy during RTD experiments

A Raman Dynisco probe (implemented in the extruder die) was connected to the Raman spectrometer (Rxn2, Kaiser Optical Systems, Washington, USA) via a fiber optical cable (position 1 in Fig 1). Raman spectra were continuously collected every 3 s with an acquisition time of 1 s once the turning valve was switched from recirculation to continuous mode. The resulting Raman spectra were SNV preprocessed to compensate for scatter-induced baseline shifts prior to the development of the RTD curve. The relative intensity of a selective Raman band (667 $cm^{-1}$) of the tracer molecule was then plotted against processing time, resulting in a RTD plot.

The residence time distribution function, e(t), is calculated as:

$$e(t) = \frac{c(t)}{\int_0^\infty c(t)dt} \quad (1)$$

where c(t)dt is the concentration of the tracer at the outlet between t and t+dt calculated from the c(t) curve (Fogler, 2006).

The degree of axial mixing is estimated by the dimensionless Peclet number (Pe). Pe was derived from the RTD plots using mean centered variance ($\sigma^2_{t_m}$) and mean residence time ($t_m$) according to the following equations:

$$\frac{\sigma^2_{t_m}}{t^2_m} = \frac{2Pe-2+2\cdot e^{-Pe}}{Pe^2} \quad (2)$$

where, mean centered variance ($\sigma^2_{t_m}$) which is measure for the width of the RTD is calculated as

$$\sigma^2_{t_m} = \frac{\int_0^\infty (t-t_m)^2 \cdot e(t)dt}{\int_0^\infty e(t)dt} \quad (3)$$

and, the mean residence time ($t_m$), describing the average exit time for the tracer to flow out the extruder once the valve was turned open (i.e., switched from recirculation mode to continues mode) is calculated as

$$t_m = \frac{\int_0^\infty t \cdot e(t)dt}{\int_0^\infty e(t)dt} \quad (4)$$

Pe is the ratio of rate of axial transport by convection and axial transport by diffusion or dispersion. In other words, high Pe values suggest a low degree of axial mixing, indicating a plug flow reactor. Plug flow is not favorable for an extrusion process since a well-mixed product (i.e., melt homogeneity) is demanded. Pe is expected to decrease (i.e., higher degree of axial mixing) with longer recirculation time of the tracer molecule in the system

environment until a plateau is reached, indicating the recirculation time needed for complete mixing of the drug in the polymer matrix (i.e., mixing endpoint).

Such a dimensionless quantification of degree of mixing can also be helpful during scaling up of the process, which is foreseen after mixing optimization at mini-extruder scale. A Pe indicating good mixing and transport in mini-extruder can be used as a benchmark to achieve similar results at the production scale.

### 2.2.4 Estimation of effects and interactions of factors

The data collected during the 49 RTD experiments (2-level full factorial design) was used to estimate the effects of the two varying factors (screw speed (100 - 200 RPM) and barrel temperature (140 - 150 °C)) upon all calculated RTD responses ($t_m$, Pe) using the Modde 10.0 software (Umetrics, Umeå, Sweden). Effect plots were calculated to show the change in the response when a factor is varied from its low level to its high level keeping the other factor at its average setting. Interaction plots were created to display the predicted change in the response when one factor varies, and the second factor is set at both its low and high level. In this plot, when both lines are parallel there is no interaction between the two factors, whereas when they cross each other there is a strong interaction.

# 3 Results and discussion

## 3.1 Influence of mini extruder process parameters upon solid-state

The spectra from the experiments performed with different concentrations (10% and 40% w/w MPT in Eudragit® RS PO) were analyzed separately as this concentration difference overwhelmed the solid state related spectral variability induced by the other varied factors (i.e., screw speed and barrel temperature). Furthermore, extrusion was not possible with 10% (w/w) MPT at 105 °C since the viscosity of the melt was too high and the maximum motor torque (18 Nm/screw) was exceeded during recirculation mode. Experiments performed at 140 °C encountered no problems as the melt viscosity decreased with increasing temperature. Also higher concentrations of MPT showed more plasticization compared to the 10% PM, hence allowing extrusion of the 40% PM at 105 °C. These observations suggest that a rheological characterization of the melt should be part of the characterization toolbox allowing to predict pharmaceutical hot-melt extrusion processability. Gupta et al. suggested that the melt viscosity of pharmaceutical hot-melt formulations should be in the range between 1000 - 10000 Pa.s (Parikh et al., 2014). Above 10000 Pa.s, the extruder motor torque would be exceeded and below 1000 Pa.s, the melt would be free flowing and not extrudable.

Fig 2 shows an interesting Raman spectral region which includes (crystalline) MPT specific peaks at 819 $cm^{-1}$ (from out of plane vibrations of COOH groups) and 847 $cm^{-1}$ (Bright et al., 2010), and also the C-C stretching vibration of Eudragit® RS PO, at 812 $cm^{-1}$ (De Veij et al., 2009).

Principal component analysis (PCA) was performed on all preprocessed spectra of the 40% API physical mixture extruded at 105 °C (at 25 and 50 RPM). The first principal component (PC1) included 88.2% of the spectral variability and distinguished between the spectra due to differences in drug crystallinity as indicated by the PC1 loadings plot (Fig 3b). Lower PC1 scores (Fig 3a) suggest a decrease in the peak intensity of the Raman peaks of MPT (at 819 and 847 $cm^{-1}$) and an increase in the peak intensity of the C-C groups from Eudragit® RS PO (Fig 2). As more MPT dissolved during processing, more amorphous and transparent product was produced and therefore the peak intensity of the C-C groups from the polymer increased. In the beginning of the process, spectra were more similar to the spectra of the physical mixtures (high PC1 scores). During processing, MPT dissolved almost completely in the matrix system until the final product was obtained (lower PC1 scores), indicated by the vertical lines in Fig 3a. The mixing endpoint was reached faster at higher screw speed as approximately 26 spectra and 50 spectra (x 5 s = recirculation time) were collected before the final product solid-state (i.e., mixing endpoint) was obtained with 50 and 25 rpm, respectively. As more MPT dissolved in the polymer melt (i.e., drug crystallinity decreased), the Raman peak intensity of the COOH vibration band decreased and simultaneously shifted, indicating O-H interactions between MPT and Eudragit® RS PO, showed in Fig 2. Furthermore, a higher screw speed resulted in a lower drug crystallinity (lower PC1 scores) due to more shear forces. Interestingly, the crystalline peaks (at 819 and 847$cm^{-1}$) of MPT did not completely disappear, indicating the production of a solid dispersion with partially crystalline and partially amorphous drug in an amorphous polymer carrier. DSC confirmed these in-line Raman findings as shown in Fig 4a. The melting enthalpy for MPT in the extrudates was smaller at 50 rpm (5.25 J/g) compared to 25 rpm (16.40 J/g), resulting in a drug crystallinity of 9% and 28%, respectively, relative to the physical mixture. These results suggest that the screw speed should be taken into account as

a significant process factor when processing below the drug melting temperature on a larger scale extruder.

PCA was also performed on the SNV preprocessed spectra (780-870 $cm^{-1}$ region) of the 10 and 40% w/w physical mixtures extruded at 140 °C. Since the Raman probe was positioned near the end of the screws (position 2), peak broadening (spectral region 780 - 870 $cm^{-1}$, shown in Fig 5) compared to the physical mixture was already observed when the molten sample passed the probes sapphire window, suggesting that MPT became amorphous or dissolved in the amorphous polymer carrier. MPT crystalline bands were no longer observed in the spectra, suggesting that amorphous MPT was obtained after extrusion of the 10 and 40% PM. DSC analysis confirmed these findings as only one Tg (i.e., glassy solid solution) and no melting peak for MPT was observed in the thermograms of extrudates containing 10 and 40% (w/w) MPT (Fig 4b). Experiments with varying screw speeds (25 - 50 rpm) could be identified based on differences in intensity of the Raman signal as indicated by the PC1 loadings plot (PC 1 = 44.1%) (Fig 6b). PC1 is related to a change in the sample presentation to the probes sapphire window linked to a different wiping effect as a function of screw speed. Other spectral variability is captured in PC2 (14.9%) and indicated the transformation of the product's solid-state during processing. The PC2 loadings plot represented melting of MPT during processing and broadening of the Raman bands, suggesting amorphization of MPT in the Eudragit® RS PO matrix. Since the PC2 scores leveled out to similar values, the final solid-state during processing is similar for both screw speeds (Fig 6a). However, this final solid-state is reached faster at higher screw speed, suggesting faster melting of MPT in the extruder with higher screw speed due to higher shear forces and faster material transport into the extruder when manual feeding was applied.

The above described results obtained with the mini extruder are compared to the former work done by Saerens et al. performed on a larger scale extruder (Prism Eurolab 16, Thermo Fisher Scientific) (Saerens et al., 2013, 2011). Saerens et al. showed that the screw speed had a significant impact on the solid-state of the extrudate when extruding a mixture containing 40% MPT at 140 °C. In that case, an increase of the screw speed from 80 to 160 rpm enabled the formation of a solid solution with a drug load of 40% (Saerens et al., 2013). In case of the mini extruder, it was possible to produce a solid solution at 140 °C with both tested screw speeds (25 and 50 rpm), using the recirculation channel. Furthermore, extrusion of the 40% (w/w) MPT physical mixture at 105°C and 80 rpm also resulted in an extrudate containing partially crystalline and partially amorphous drug in the amorphous carrier as described in (Saerens et al., 2011). Increasing the screw speed from 80 to 160 rpm at 100 °C did not change the final solid-state of the extrudate as described in (Saerens et al., 2013). Increasing the screw speed only changed the location of the barrel section where the final solid-state was produced. This is in contrast with the results from the mini extruder since a change in the drug crystallinity was observed when extrusion was performed below the drug melting point with a higher screw speed.

### 3.2 Residence time analysis

Table 1 lists the results from the RTD experimental setup. A DOE analysis was performed for each response ($t_m$ and Pe) at each recirculation time in order to elucidate the effect of the studied factors (barrel temperature and screw speed) upon the responses ($t_m$, Pe). Since the variability for the $t_m$ response was low in this experimental set up at 0 and 15 s recirculation

time, no good MLR models could be built. Figure 7 shows the effect plots for $t_m$ at varying tracer recirculation times (30, 45, 60 and 90 s). The influence of screw speed on $t_m$ is straightforward. A lower screw speed resulted in a longer $t_m$ at every tracer recirculation time. Barrel temperature had no significant effect upon $t_m$ at low tracer recirculation times (e.g. 30, 45, 60 s). However, using longer mixing times (e.g. Fig 7, 90 s tracer recirculation time) of the tracer with the polymer, a higher barrel temperature slightly decreased the exit time of the product from the barrel (i.e., shorter $t_m$). This observation was linked to a temperature effect on the viscosity of a well-mixed product. After 90 s, the viscosity of the mixture (tracer + polymer) has stabilized, which can be seen from the force measurements in the extruder. With lower process temperatures, the viscosity of the mixture increased and resulted in a prolonged $t_m$. The interaction plot (Fig 7b) shows a significant interaction (i.e., no parallel lines) for $t_m$ between the barrel temperature and screw speed after longer tracer recirculation times (90 s). At high screw speeds, transport of melt from the system is not significantly influenced by the barrel temperature. This observation is due to the shear thinning effect of polymer melts at higher screw speeds (Kohlgrüber, n.d.). On the other hand, a low screw speed in combination with a higher barrel temperature resulted in faster discharge of the material from the extruder (i.e., lower $t_m$) compared to a low screw speed and low barrel temperature. This observation can be explained by the higher melt viscosity at low screw speed (i.e., lower shear rate) and low temperature compared to the melt viscosity at low screw speed and higher temperature.

Figures 8 a and b show Pe as a function of tracer recirculation time (0 - 90 s) for the experiments performed at 140 °C and 150 °C, respectively. As expected, Pe decreased with a longer recirculation time until a plateau region is reached, indicating the mixing endpoint. These plots illustrate that the mixing endpoint (i.e., Pe plateau value) was reached faster at

higher screw speed. However, giving sufficient tracer recirculation time, all experimental setups reached a similar plateau level, suggesting that homogeneous melts are obtained. From the moment Pe reached the plateau value, the barrel temperature and screw speed had no significant effect upon Pe. When increasing the screw speed (100 to 200 rpm) at a low temperature (140°C) at 0 s recirculation time, axial mixing was observed to reduce drastically. Furthermore, Fig 9a shows the effect plot for Pe when the tracer molecule was not circulated (i.e., 0 s recirculation time). An interaction is clearly observed between screw speed and barrel temperature (Fig 9b). The effect of screw speed is different at the two levels of temperature. At a high screw speed, a large effect of temperature is seen, whereas at a low screw speed, there is no effect of temperature. At a low temperature (140 °C) and a high screw speed (200 rpm), frictional forces were easily overtaken by drag force leading to low degree of axial mixing (i.e., high Pe), indicating a plug flow regime (Fig 10). This result suggested that temperature driven viscosity reduction and longer recirculation times were equally needed for the tracer to be homogenously mixed. On the other hand, Pe is lower at a low screw speed and high barrel temperature. This interaction suggests that a simultaneous increase in temperature and screw speed improved the axial mixing degree due to softening of the material (melt viscosity decreases at higher temperature). The axial mixing, which involves transport of melt through the clearance between screws and barrel is driven by the ratio of the drag force by the screws and the viscous force of the melt resisting the drag force. At a low screw speed, the axial mixing degree is less affected by the barrel temperature because the residence time in the extruder is longer and the significance of the shear thinning effect is low.

# 4 Conclusion

In-line Raman spectroscopy was used in combination with a vertical mini extruder. This combination has shown to be beneficial for fast screening of new pharmaceutical melt formulations. In this study, the influence of important process parameters (screw speed and barrel temperature) upon the solid-state transformation of a sustained release formulation during processing in recirculation mode was examined. Processing below the drug melting point (105 °C) with higher screw speed (50 rpm) resulted in a lower drug crystallinity due to higher shearing forces. Also a faster mixing endpoint was obtained at higher screw speed. Processing above the melting point of the crystalline drug (140°C) resulted in the formation of a solid solution at both low (25 rpm) and high screw speed (50 rpm) during processing. The chemical information obtained with in-line Raman spectroscopy during processing in a mini extruder can be taken into account during up-scaling. Furthermore, RTD measurements elucidated the improved mixing capacity when using the mini extruder's recirculation channel compared to running in continuous mode (i.e., 0 s tracer recirculation time). Higher screw speeds resulted in a faster mixing endpoint and transport from the system. The barrel temperature was only significant when sufficient recirculation time (90 s) was allowed to equilibrate the viscosity during processing. At high screw speeds, the transport from the extruder was not significantly different between low and high barrel temperature due to the shear thinning effect. However, at low screw speeds, faster transport was observed at higher barrel temperature, linked to the lower melt viscosity. Since the melt viscosity is important for future processability, rheological characterization of the melt properties should be included in future research.

## Acknowledgments

Acknowledgements for Xplore Instruments for providing the specialized equipment and technical support.

## References

Administration, U.S.F. and D., 2004. Guidance for industry: PAT — a framework for innovative pharmaceutical development, manufacturing, and quality assurance. U.S. Dep. Heal. Hum. Serv. 1–16.

Bright, A., Renuga Devi, T.S., Gunasekaran, S., 2010. Spectroscopical vibrational band assignment and qualitative analysis of biomedical compounds with cardiovascular activity. Int. J. ChemTech Res. 2, 379–388.

Common, A., Rodier, E., Sauceau, M., Fages, J., 2014. Flow and mixing efficiency characterisation in a CO2-assisted single-screw extrusion process by residence time distribution using Raman spectroscopy. Chem. Eng. Res. Des. 92, 1210–1218. doi:10.1016/j.cherd.2013.10.013

De Beer, T., Burggraeve, a., Fonteyne, M., Saerens, L., Remon, J.P., Vervaet, C., 2011. Near infrared and Raman spectroscopy for the in-process monitoring of pharmaceutical production processes. Int. J. Pharm. 417, 32–47. doi:10.1016/j.ijpharm.2010.12.012

De Veij, M., Vandenabeele, P., De Beer, T., Remon, J.P., Moens, L., 2009. Reference database of Raman spectra of pharmaceutical excipients. J. Raman Spectrosc. 40, 297–307. doi:10.1002/jrs.2125

Fogler, H.S., 2006. Distributions of residence times for chemical reactors. Elem. Chem. React. Eng. 867–944.

Islam, M.T., Scoutaris, N., Maniruzzaman, M., Moradiya, H.G., Halsey, S. a, Bradley, M.S. a, Chowdhry, B.Z., Snowden, M.J., Douroumis, D., 2015. Implementation of transmission NIR as a PAT tool for monitoring drug transformation during HME processing. Eur. J. Pharm. Biopharm. 96, 106–16. doi:10.1016/j.ejpb.2015.06.021

Kohlgrüber, K., n.d. Twin-screw extruders.

Parikh, T., Gupta, S.S., Meena, A., Serajuddin, A.T.M., 2014. Investigation of thermal and viscoelastic properties of polymers relevant to hot melt extrusion - III : Polymethacrylates and polymethacrylic acid based polymers . J. Excipients Food Chem 5, 56–64.

Saerens, L., Dierickx, L., Lenain, B., Vervaet, C., Remon, J.P., Beer, T. De, 2011. Raman spectroscopy for the in-line polymer-drug quantification and solid state characterization during a pharmaceutical hot-melt extrusion process. Eur. J. Pharm. Biopharm. 77, 158–163. doi:10.1016/j.ejpb.2010.09.015

Saerens, L., Dierickx, L., Quinten, T., Adriaensens, P., Carleer, R., Vervaet, C., Remon, J.P., De Beer, T., 2012. In-line NIR spectroscopy for the understanding of polymer-drug interaction during pharmaceutical hot-melt extrusion. Eur. J. Pharm. Biopharm. 81, 230–237. doi:10.1016/j.ejpb.2012.01.001

Saerens, L., Vervaet, C., Remon, J.-P., De Beer, T., 2013. Visualization and process understanding of material behavior in the extrusion barrel during a hot-melt extrusion process using Raman spectroscopy. Anal. Chem. 85, 5420–9. doi:10.1021/ac400097t

Sakai, T., Thommes, M., 2014. Investigation into mixing capability and solid dispersion preparation using the DSM Xplore Pharma Micro Extruder. J. Pharm. Pharmacol. 66, 218–231.

Verreck, G., Decorte, A., Heymans, K., Adriaensen, J., Liu, D., Tomasko, D., Arien, A., Peeters, J., Van den Mooter, G., Brewster, M.E., 2006. Hot stage extrusion of p-amino salicylic acid with EC using CO2 as a temporary plasticizer. Int. J. Pharm. 327, 45–50. doi:10.1016/j.ijpharm.2006.07.024

Vigh, T., Drávavölgyi, G., Sóti, P.L., Pataki, H., Igricz, T., Wagner, I., Vajna, B., Madarász, J., Marosi, G., Nagy, Z.K., 2014a. Predicting final product properties of melt extruded solid dispersions from process parameters using Raman spectrometry. J. Pharm. Biomed. Anal. 98, 166–177. doi:10.1016/j.jpba.2014.05.025

Vigh, T., Sauceau, M., Fages, J., Rodier, E., Wagner, I., Sóti, P.L., Marosi, G., Nagy, Z.K., 2014b. Effect of supercritical CO<inf>2</inf> plasticization on the degradation and residual crystallinity of melt-extruded spironolactone. Polym. Adv. Technol. 25, 1135–1144. doi:10.1002/pat.3367

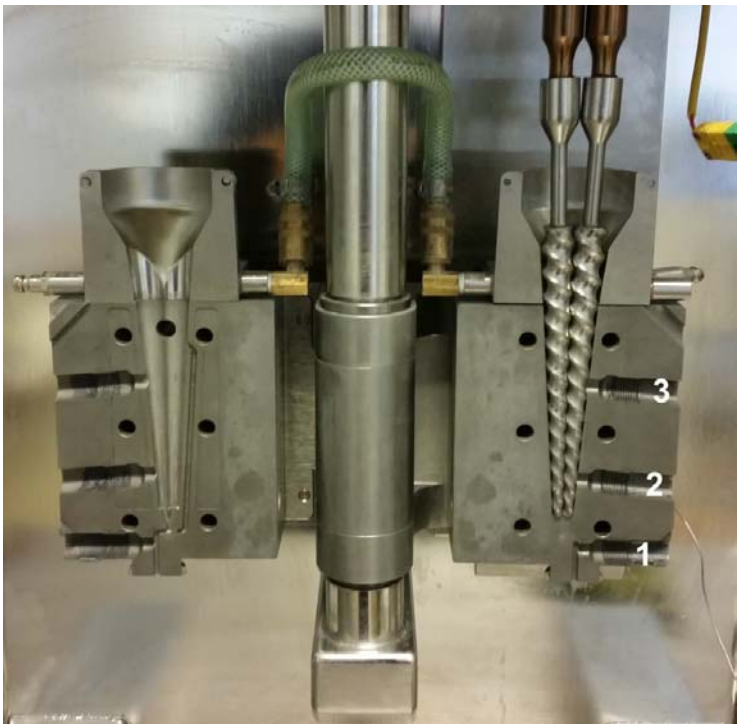


Figure 1: PME 5 with splittable, removable barrel liners. Three implementation zones for the Raman Dynisco probe: 1) In the extruder die 2) lowest position against the screws 3) highest position against the screws.

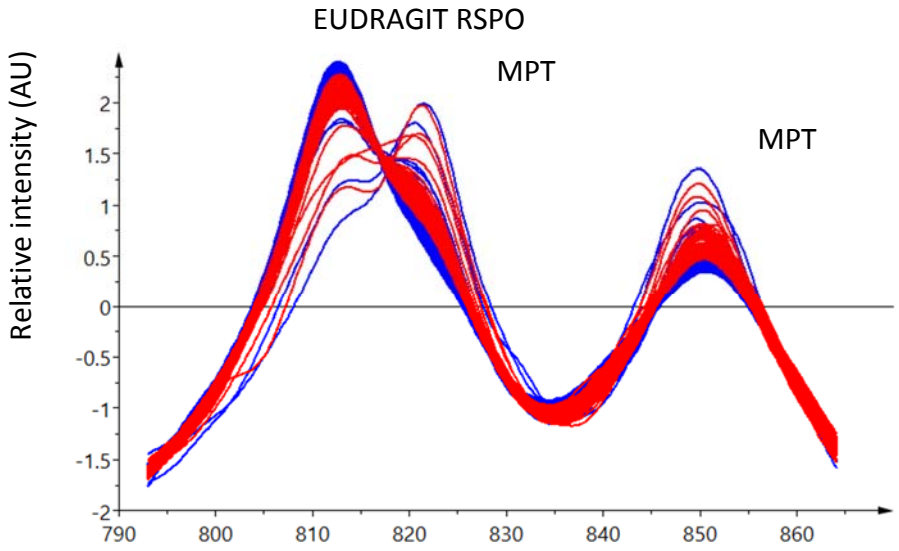


Figure 2: In-line Raman spectra of the melt collected during extrusion of the 40% (w/w) MPT physical mixture at 105 °C, red: 25 rpm, blue: 50 rpm.

a)

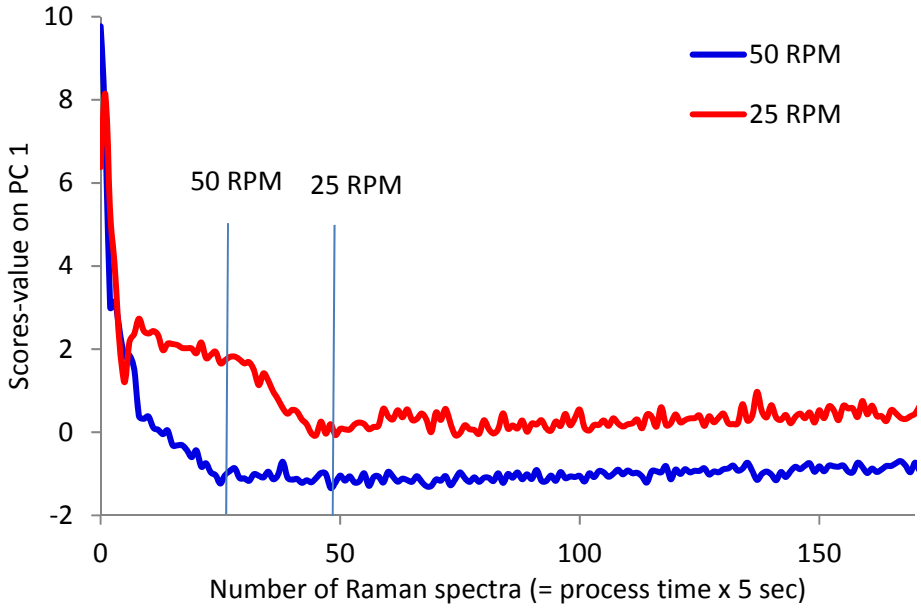


b)

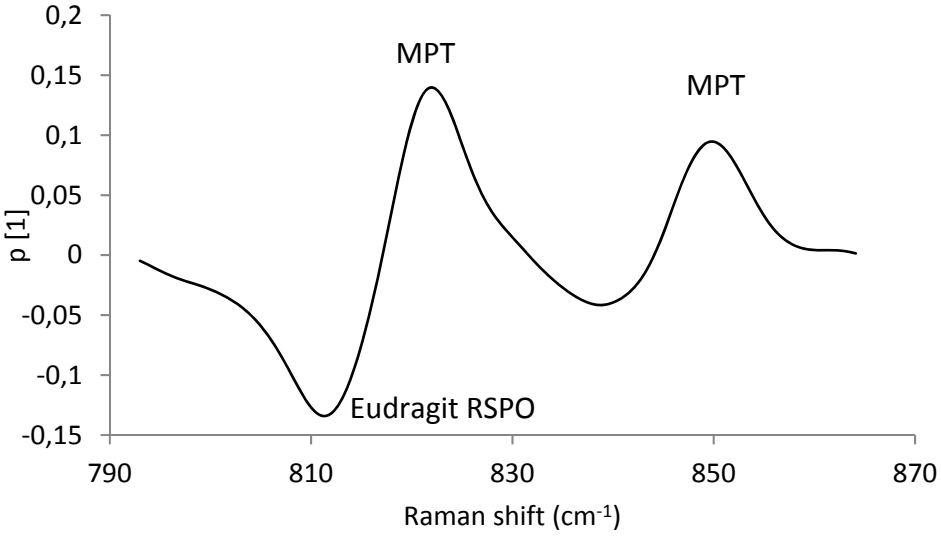


Figure 3: a) PC1 scores in function of progression of spectral data collection (i.e., processing time). The vertical lines indicate when the final solid-state of the product is obtained with 25 rpm (red) and 50 rpm (blue). b) Loading plot of the first principal component.

a)

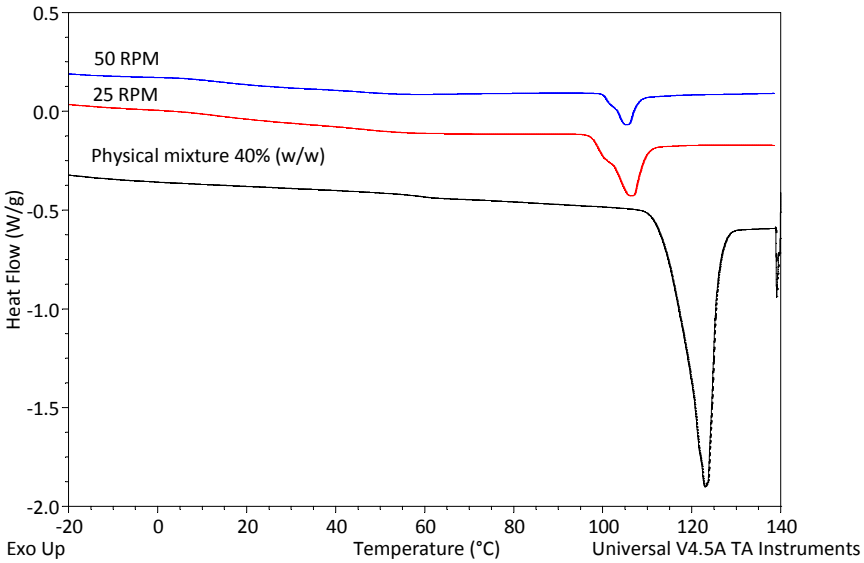


b)

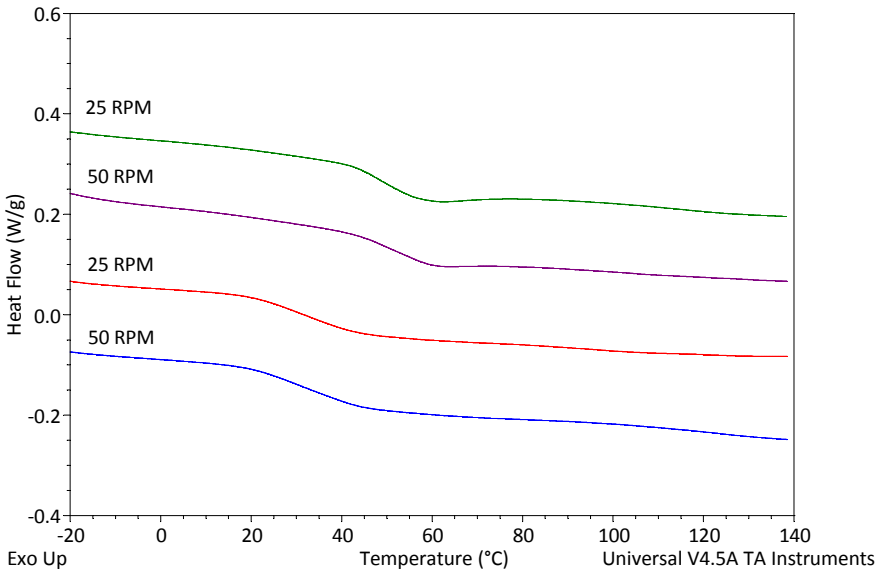


Figure 4: a) Thermograms of the extrudates after extrusion at 105 °C of a 40% MPT (w/w) physical mixture at 25 rpm (red) and 50 rpm (blue). b) Thermograms of the extrudates after extrusion at 140 °C of a 40% (w/w) MPT physical mixture at 25 rpm (red) and 50 rpm (blue) and of a 10% (w/w) MPT physical mixture at 25 rpm (green) and 50 rpm (purple).

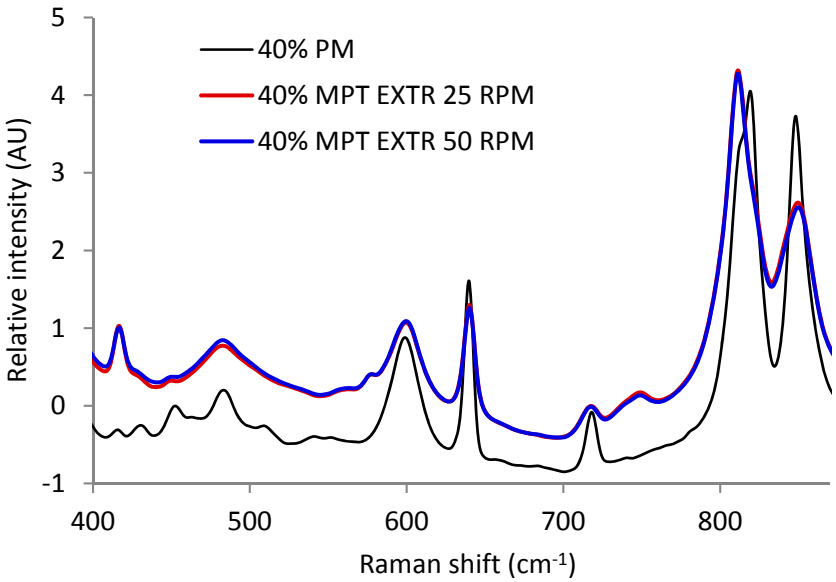


Figure 5: Comparison between physical mixture and in-line collected spectra during extrusion of a 40% PM at 140 °C, 25 rpm (red) and 50 rpm (blue).

a)

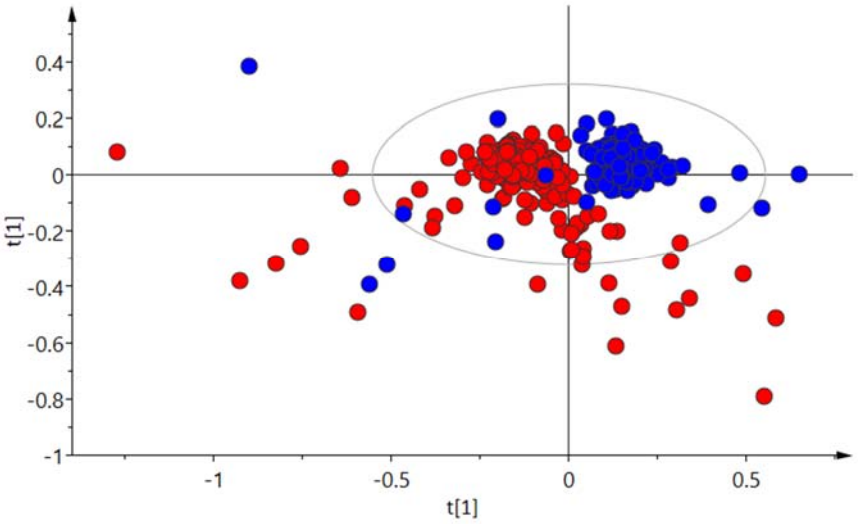


b)

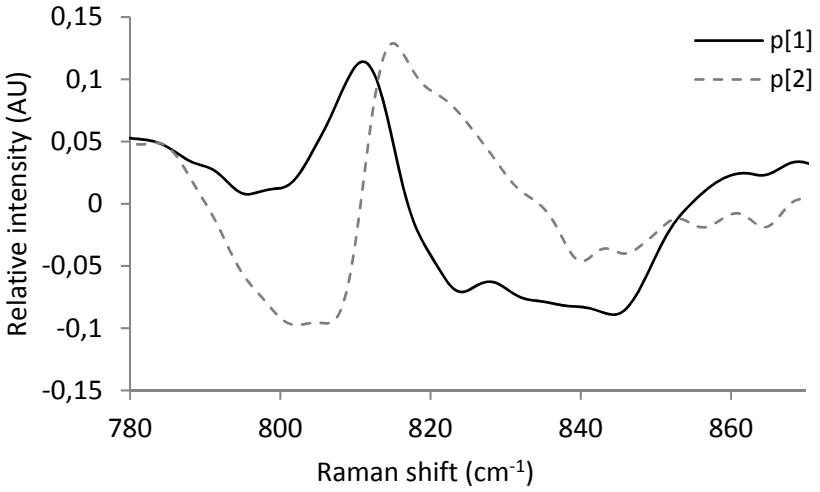


Figure 6: a) PC 1 vs PC 2 scores scatter plots of in-line collected Raman spectra during extrusion (at 140°C) of a 40% physical mixture at 25 rpm (red) and 50 rpm (blue); b) PC 1 (solid) and PC 2 (dashed) loadings plot.

a)

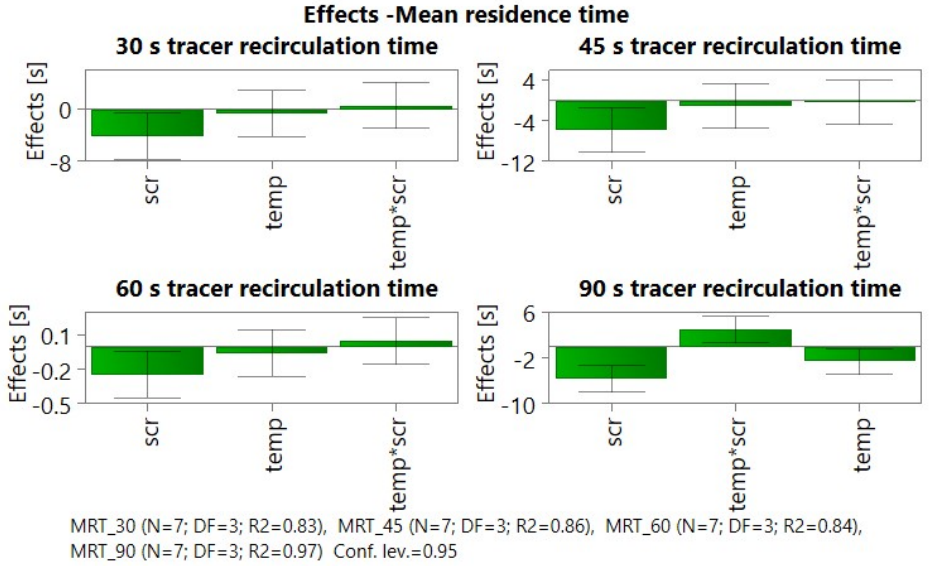


b)

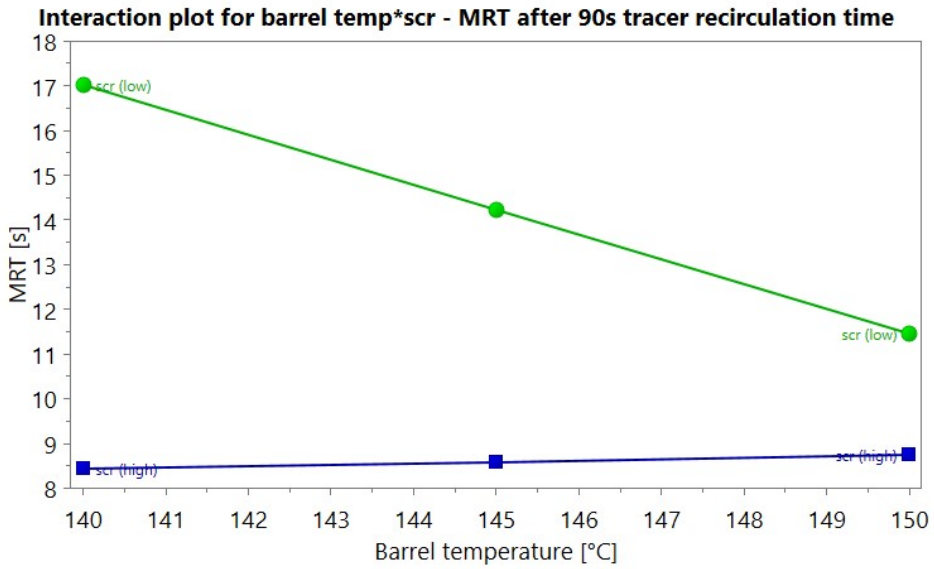


Figure 7: a) Effect plots for mean residence time, $t_m$, at tracer recirculation times of 30, 45, 60 and 90s. b) Interaction plot for barrel temperature and screw speed upon $t_m$ after 90 s tracer recirculation time.

a)

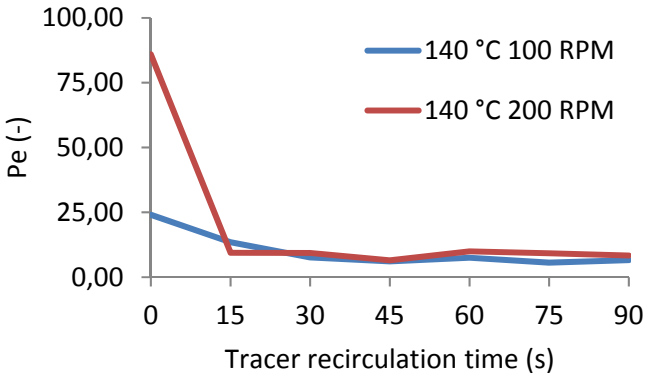


b)

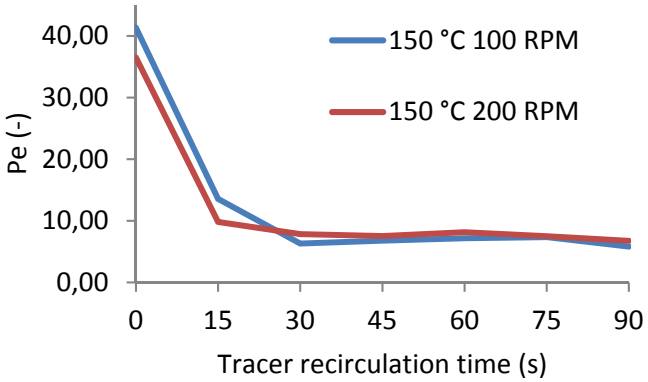


Figure 8: Peclet number in function of tracer recirculation time for experiments at 140 °C (a) and 150 °C (b).

a)

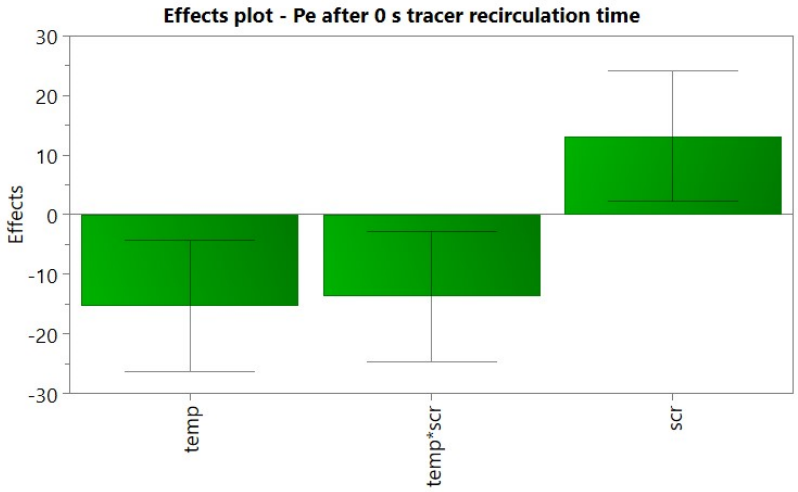


b)

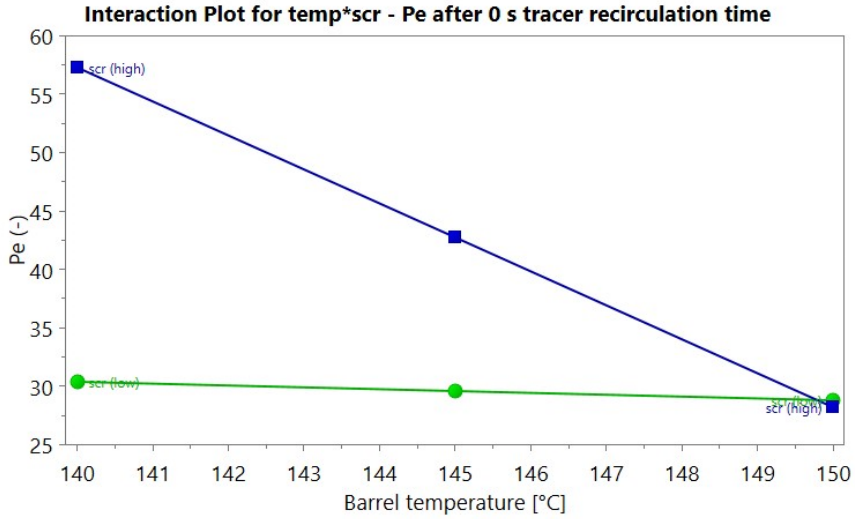


Figure 9: a) Effect plot for Pe after 0 s tracer recirculation time. b) Interaction plot for barrel temperature and screw speed upon Pe after 0 s tracer recirculation time.

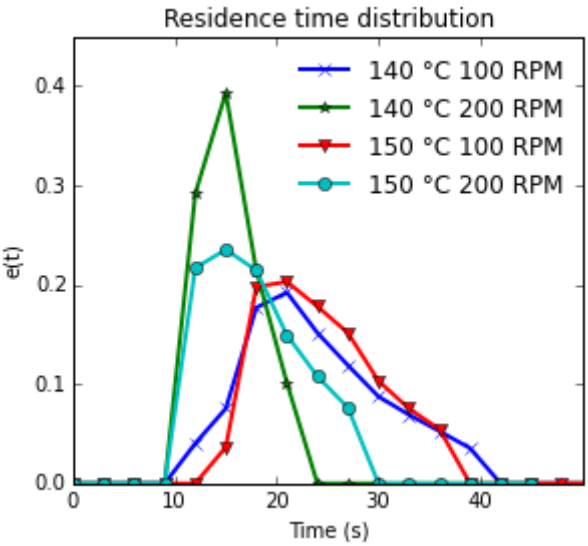


Figure 10: Residence time distribution plots of experiments performed at 0 s tracer recirculation time in function of screw speed and barrel temperatures.

| Barrel temperature (°C) | Screw speed (RPM) | Tracer recirculation time (s) | | | | | | | | | | | | | |
|---|---|---|---|---|---|---|---|---|---|---|---|---|---|---|---|
| | | 0 | 15 | 30 | 45 | 60 | 75 | 90 | 0 | 15 | 30 | 45 | 60 | 75 | 90 |
| | | Mean residence time (s) | | | | | | | Peclet number (-) | | | | | | |
| 140 | 100 | 26.9 | 15.5 | 15.6 | 15.1 | 16.7 | 16.8 | 17.2 | 30.8 | 13.5 | 7.6 | 6.1 | 7.5 | 5.6 | 6.6 |
| 150 | 100 | 24.4 | 16.5 | 14.3 | 14.4 | 13.1 | 10.2 | 11.7 | 29.2 | 13.6 | 6.3 | 6.8 | 7.2 | 7.4 | 5.8 |
| 140 | 200 | 15.4 | 9.3 | 10.9 | 9.6 | 8.5 | 10.7 | 8.7 | 57.7 | 9.4 | 9.4 | 6.5 | 10.0 | 9.2 | 8.3 |
| 150 | 200 | 17.8 | 9.0 | 10.7 | 8.2 | 8.3 | 10.0 | 9.0 | 28.7 | 9.8 | 7.9 | 7.5 | 8.2 | 7.5 | 6.8 |
| 145 | 150 | 14.4 | 8.7 | 13.0 | 10.4 | 9.8 | 11.2 | 11.1 | 36.9 | 9.2 | 8.4 | 7.6 | 8.4 | 9.2 | 7.9 |
| 145 | 150 | 14.5 | 9.5 | 10.8 | 10.0 | 8.8 | 11.2 | 10.4 | 38.9 | 9.8 | 4.5 | 7.3 | 10.0 | 11.4 | 8.6 |
| 145 | 150 | 17.7 | 9.1 | 12.8 | 9.7 | 12.0 | 10.6 | 11.9 | 31.0 | 9.3 | 7.8 | 8.1 | 6.7 | 8.6 | 6.7 |

Table 1: RTD results of the full factorial design with 2 factors (screw speed - barrel temperature) at 2 levels for 7 tracer recirculation times.